

# Experimental Study on Mixed Mode Crack Propagation

ZHAO YISHU

*Department of Mechanics, Huazhong University of Science and Technology, Wuhan, PRC*

## ABSTRACT

The cracked specimens which are made of four kinds of brittle material have been tested under all possible combination of Modes I, II and III. On the basis of measured data, an empirical criterion of mixed mode crack propagation is suggested. The effect of coupling between  $K_1$  and  $K_3$  on the fracture mechanism and fracture toughness of materials is discussed in macroscopic and microscopic ways.

## KEYWORDS

Coupling action; fracture toughness; mixed mode fracture; intergranular fracture; parabolical dimple.

## INTRODUCTION

According to linear elastic fracture mechanics developed by Irwin (Irwin, 1957), stress intensity factor  $K$  can be used as a simple scalar parameter to describe elastic stress field near the crack tip. In classical failure theory, it is assumed that the critical value of certain mechanical parameter under the combined loading, which is taken as the failure standard of the material, should be the same value obtained in the uniaxial tension test. Similarly, in the linear elastic fracture mechanics, it is supposed that the critical value for mixed mode fracture criterion could be obtained from the critical stress intensity factor  $K_{Ic}$  of Mode I crack. But the experimental results indicate that the stress intensity factor  $K_1$  at fracture (denoted by  $K_{1f}$ ) may be greater than the fracture toughness  $K_{Ic}$  if the combined loading involves Mode I and III at the same time. The maximum value of the ratio  $K_{1f}/K_{Ic}$  may be as high as 1.85. Thereby the capability of the resistance to fracture is significantly increased. Although the above mentioned coupling effect of Mode I and III also appeared in the tests of other investigators (Shah, 1974, Ueda et al., 1983, Wilson et al., 1968) for many years, it has been ignored. This problem will be discussed through the analysis of the measured data and the inspection of the fracture surface in this paper.

EXPERIMENTS

The fracture tests of pure mode I, II and III as well as all their possible combinations have been performed under the condition of normal temperature and static loading. The experimental technique which was used by Chell et al. (Chell et al., 1978) has been used in the tests. The specimens were made of W18Cr4V, 60Si2Mn and 2Cr13 steel and PMMA respectively. The specimens were heat treated to a high hardness with a low fracture toughness. The configuration of the specimens is shown in Fig.1. A straight notch 15mm in length was cut at the edge of the specimen by using an electric discharge machine.

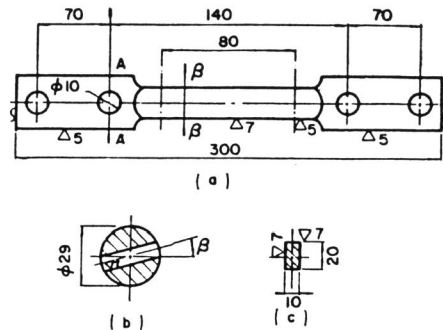


Fig.1 Cracked specimen

The standard fatigue pre-cracking procedure was employed to obtain a sharp crack. The specimen is connected to the loading apparatus which is mounted on to an universal testing machine. Various loading types with different values of  $\alpha$  and  $\beta$  (see Fig.2) are considered.  $\alpha$  denotes the angle between longitudinal axis of the specimen and horizontal line, and  $\beta$  is the rotating angle of the specimen about its own axis. The magnitudes of  $\alpha$  and  $\beta$  are regulated by the loading apparatus and four circular holes in the specimen respectively. The specimen will be subjected to pure Mode I, II and III loading when  $\alpha=90^\circ, \alpha=\beta=0$  and  $\alpha=0, \beta=90^\circ$  respectively:

TEST RESULTS

Mode I-II test

The stress intensity factors are (Chell et al., 1978)

$$K_1 = \sigma \sin \alpha \sqrt{a} Y_1(a/w), K_2 = \sigma \cos \alpha \sqrt{a} Y_2(a/w). \quad (1)$$

Fig.3 shows the Fracture Envelope plotted according to the test points under combined Mode I-II loading. The Fracture Envelope equation may be obtained by using Scarborough's (Scarborough, 1955) method that determines empirical formula from the experimental curve as follows

$$0.05(K_1/K_{1c})^2 + 0.95(K_1/K_{1c}) + 2.16(K_2/K_{1c})^2 = 1 \quad (2)$$

The average value of the ratio  $K_{1f}/K_{1c}$  of four kinds of material from the test under pure Mode I and II loading is 0.68.

Mode II-III test

The stress intensity factors are (Chell et al., 1978)

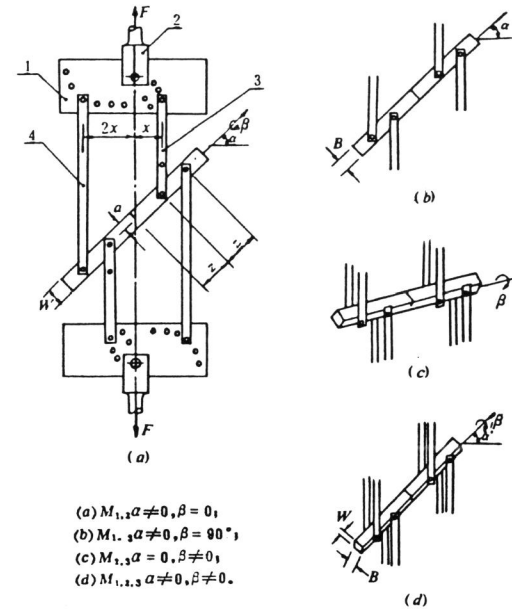


Fig.2 Mixed modes loading state.

$$K_2 = \sigma \cos \beta \sqrt{a} Y_2(a/w), K_3 = \sigma \sin \beta \sqrt{a} Y_3(a/w). \quad (3)$$

Fig.4 shows the Fracture Envelope which is plotted according to the test points under the combined Mode II-III loading. The Fracture Envelope equation may be obtained also by using Scarborough's (Scarborough, 1955) method as follows

$$2.16(K_2/K_{1c})^2 + 1.98(K_3/K_{1c})^2 \quad (4)$$

The average value of the ratio  $K_{3f}/K_{1c}$  of four kinds of material from the test under pure Mode III loading is 0.71.

Mode I-III test

The stress intensity factors are (Chell et al., 1978)

$$K_1 = \sigma \sin \alpha \sqrt{a} Y_1(a/w), K_3 = \sigma \cos \alpha \sqrt{a} Y_3(a/w). \quad (5)$$

The average ratio  $K_{1f}/K_{1c}$  of four kinds of material in our tests versus the angle  $\alpha$  is plotted in Fig.5 by broken line. The theoretical curve of  $K_{1f}/K_{1c}$  versus the angle  $\alpha$  is a sine curve by solid line in Fig.5. From Fig.5 we see that  $K_{1f}$  must be less or equal to  $K_{1c}$ . But the test results indicate that  $K_{1f}$  is always greater than  $K_{1c}$  if Mode I component exceed a certain value and

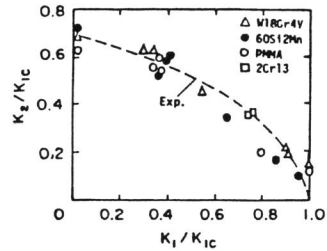


Fig.3 Test points and Fracture Envelope under mixed Mode I-II.

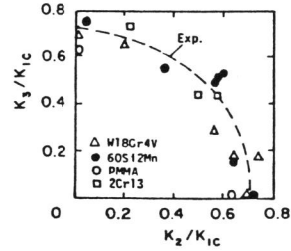


Fig.4 Test points and Fracture Envelope under mixed Mode II-III.

the ratio  $K_{1f}/K_{1c}$  will increase as  $\alpha$  increases. It implies that the greater the  $K_1$  component is the more it is sensitive to the coupling action of  $K_2$ . This is because the angle  $\alpha$  is the parameter which dominates the magnitude of  $K_1$  component and the larger the  $\alpha$  the greater the  $K_1$  component.

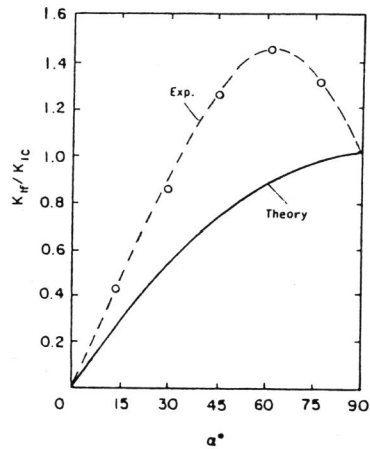


Fig.5  $K_{1f}$  VS fracture angle

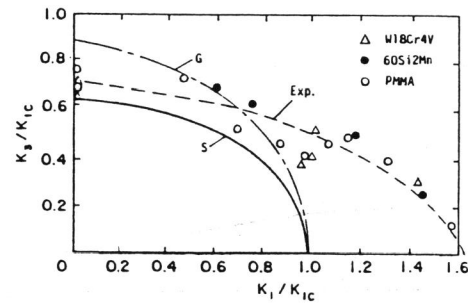


Fig.6 Comparison between predicted and test results under mixed Mode I-III fracture

According to eqs.(2) and (4) the Fracture Envelope equation of mixed Mode I-III may be obtained as follows

$$0.05(K_1/K_{1c})^2 + 0.95(K_1/K_{1c}) + 1.98(K_3/K_{1c})^2 = 1 \quad (6)$$

and it was plotted in Fig.6. Fig.6 also gives the Fracture Envelope predicted by the strain energy density criterion (S-criterion) (Sih,1974) and the data

from mixed Mode I-III fracture test.

About half of the test points are located in the right side of the abscissa 1.0 at the coordinate axis. It will be questionable if  $K_{1c}$  is still considered as a constant representing material behaviour and is regarded as the standard of mixed mode fracture criteria because the fracture toughness is risen obviously due to the coupling effect of  $K_1$  and  $K_3$ .

#### Mode I-II-III test

The stress intensity factors are

$$\begin{aligned} K_1 &= \sigma \sin \alpha \sqrt{a} Y_1(a/w), & K_2 &= \sigma \cos \alpha \cos \beta \sqrt{a} Y_2(a/w), \\ K_3 &= \sigma \cos \alpha \sin \beta \sqrt{a} Y_3(a/w). \end{aligned} \quad (7)$$

The first of eqn.(7) shows that  $K_{1f}$  is independent of the angle  $\beta$  and depends only on the angle  $\alpha$  for mixed Mode I-II-III fracture. This, in fact, implies that Mode III loading has no effect on the value  $K_{1f}$  because of the angle  $\beta$  dominating the level of Mode III loading. Therefore, the ratio  $K_{1f}/K_{1c}$  versus the angle  $\alpha$  must be a sine curve in  $K_{1f}/K_{1c} - \alpha$  orthogonal coordinate system. However, the test results show that the  $K_{1f}$  value will increase with increasing  $\beta$ . This means that the  $K_{1f}$  value will increase with increasing the component of Mode III loading. Fig.8 shows that  $K_{1f}$  is independent of the angle  $\beta$  only when  $\alpha < 15^\circ$  or  $K_{1f}/K_{1c} < 0.40$ . Fig.7 and 8 also show that  $K_{1f}$  can be greater than  $K_{1c}$  when  $\alpha > 45^\circ$  or  $\beta > 45^\circ$ . The  $K_{1f}$  value is always greater than  $K_{1c}$  when both  $\alpha$  and  $\beta$  are greater than  $45^\circ$ . It implies that the greater the  $K_1$  value the more the susceptible of  $K_1$  to the coupling action of  $K_3$ . The  $K_{1f}$  value under mixed Mode I-II-III is always greater than the  $K_{1c}$  for high level of the component of Mode I and III loading.

The empirical equation of the Fracture Envelope for mixed Mode I-II-III may be obtained from eqn.(2) and (4) as follows

$$0.05(K_1/K_{1c})^2 + 0.95(K_1/K_{1c}) + 2.16(K_2/K_{1c})^2 + 1.98(K_3/K_{1c})^2 = 1 \quad (8)$$

An ellipsoidal surface in  $K_1/K_{1c} - K_2/K_{1c} - K_3/K_{1c}$  Cartesian orthogonal space is defined by eqn.(8). This ellipsoidal surface can be expressed as a set of elliptical curve in three projection planes of the first quadrant in Cartesian orthogonal space. They were plotted in Fig.9.

#### INSPECTION OF FRACTURE SURFACES

##### Microstructure

The fracture surfaces of Mode I and II appeared granular with smooth facets. The difference between Mode I and II fracture surface only is that the former will propagate in a coplanar fashion, but the latter will propagate with an angle of  $65^\circ$  to  $70^\circ$  to the original crack plane. The fracture surface of Mode I-II and Mode I is similar in shape. Mode II-III fracture surface is a curvi-plane in space. Apparent deformation before fracture for the four kinds of specimens has not been observed.

The fracture corresponding to Mode III loading has been assumed to grow in a coplanar fashion as extension of Mode I crack which is in contrast to the

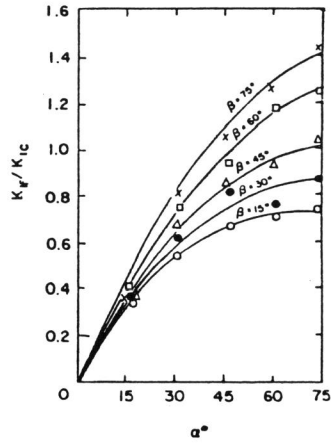


Fig. 7  $K_{If}$  VS fracture angle  $\alpha$  under mixed Mode I-II-III fracture.

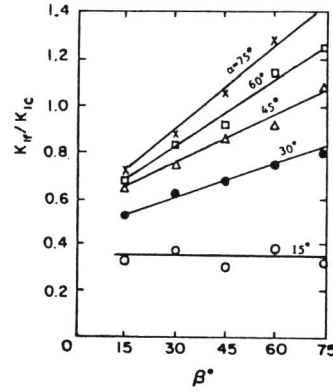


Fig. 8  $K_{If}$  VS angle  $\beta$  under mixed Mode I-II-III fracture.

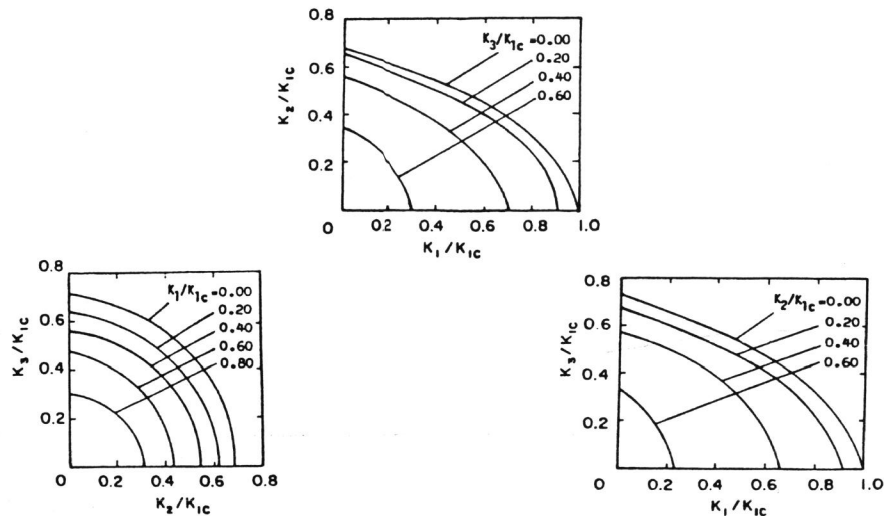


Fig. 9 Fracture Envelope predicted by empirical criterion for mixed Mode I-II-III crack propagation

experimental results obtained here. Thus Mode I-III crack extension was considered to be also in coplaner fashion. In fact, an initial Mode III crack extension was followed by Mode I crack branching. Mode III fracture surface is curved in shape which resemble that occurring in pure torsion. It is in accordance with Tsangarkis (Tsangarakis, 1984) test results obtained by use of the circumferentially cracked round bars. The mechanism of the formation of

Mode I crack branch from a Mode III type crack under Mode III lading have been studies by Pook (Pook et al., 1979). The postulates presented by Pook, can not explain why Mode I crack branching does not take place in some steel. A possible explanation was suggested by Tsangarkis (Tsangarkis, 1984). All of Mode I-III fracture surface presented screw curvi-plane from our test results. It was found that there is a rough fibrous region in front of the precrack and hold radiated tear ridge neighboured with the fibrous region on the screw curvi--lane. It indicates that the fracture process was accompanied by large plastic deformation, and correspond with twisting deformation of the specimens and the necking near the crack tip before fracture under combined Mode I-III loading. There is a granular smooth facet neighbouring with radiated tear ridge except the existence of fibrous region and radiated tear ridge on fracture surface of Mode I-II-III. They were caused by brittle shear because of presence of Mode II.

#### Fractographies

Fig. 10 and 11 are scanning electron fractographies of 60Si2Mn steel. Fig. 10 is the case of pure Mode I fracture, Fig. 11 is the case of mixed Mode I-II-III fracture. According to "Rock Candy" fractography in Fig. 10, puer Mode I fracture pertains to typical intergranular fracture. But parabolical dimples are appeared in Fig. 11. This may be attributed to the coupling effect of Mode I and III which caused larger plastic deformation under the combined Mode I-II-III fracture.

#### DISCUSSION

Mode I fracture pertains to tensile fracture and gives rise to triaxial stress state ahead of crack tip. Although Mode II and III fracture are all shear failure, but both types of failure are not the same in respect of macroscopic deformation and microscopic mechanism. Mode II fracture produces direct shearing deformation and is similar to the edge dislocation in the motion fashion. Mode III fracture produces twisting deformation and is similar to the screw dislocation in the motion fashion. Mode III loading is actually torsional load and the distribution of shearing stress will be made to follow the triangle law in the section of the specimen. Maximum shearing stress presents at the edge of the section. The value of shearing stress is zero in the centroid of the section. Since triaxial stress field near crack tip under Mode I loading is susceptible to shearing strain, thus a part of material ahead of crack tip yielded first and led to local plastic deformations due to maximum shearing stress, then the necking is caused by tensile stresses. That is why the necking can be formed near the crack tip under combined Mode I-II

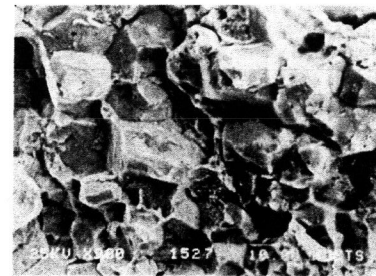


Fig. 10 Pure Mode I fracture

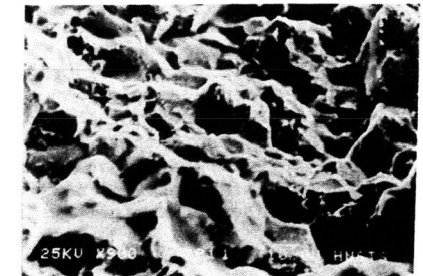


Fig. 11 Mixed Mode I-II-III fracture

and I-II-III loading. The necking region is virtually a smooth breach. A biaxial traverse tensile stress state was caused by Mode I loading ahead of the crack tip. It increased the value of axial stress necessary for causing plastic flow. This value of the increased stress has been analysed and calculated by Bridgman (Bridgman, 1944). The breach effect of necking region increased fracture toughness of materials and led to brittle fracture with local plastic deformation.

Though the distribution of shearing stress due to direct shear in the section of the specimen has been not revealed yet, but it is proved from the theory of elasticity that the value of shearing stress near crack tip is zero. Therefore, the local stress field near the crack tip reaches the tensile strength before it reaches shearing strength under the combined Mode I-II loading, thereby led to sole brittle fracture. The necking is not formed near crack tip when Mode II and III loading are only involved because the component of Mode I loading is not present. Therefore, fracture toughness can not be increased under mixed Mode I-II and II-III fracture.

#### REFERENCES

- Sih, G.C. (1974). Strain-energy-density factor applied to mixed mode crack problems, int. J. Fracture 10, 305-321.
- Shah, R.C. (1974). Fracture under combined mode in 4340 steel. ASIM STP560, 29-52.
- Ueda, Y. K.Ikeda, T.Yao and M.Aoki (1983). Characteristic of brittle fracture under general combined mode including those under biaxial tensile loads. Engng Fracture Mech. 18, 1131-1158.
- Irwin, G.R. (1957). Analysis of stresses and strains near the end of crack transversing a plane. J.Appl Mech. 24, 361-364.
- Wilson, W.K. W.G.Clark and E.T.Wossel (1968). Fracture mechanics technology for combined loading, Low to Intermediate strength metals. AD682754.
- Chell G.G. and E.Cirvan (1978). An experimental technology for fast fracture testing in mixed mode. Int.J.Fracture 14, R81-R84.
- Scarborough, J. B. (1955). Numerical mathematical analysis. Third Edition.
- Tsangarakis, N. (1984). The dependence of Mode III fracture initiation toughness on strength and microstructure. Engng fracture Mech. 19, 903-909.
- Pook L.P. and J.K.Sharple (1979). The Mode III fatigue crack growth threshold for mild steel. Int.J Fracture 15, R225-R226.
- Bridgman, P.W. (1944). Trans. Am. Soc. Met. 32, 553.